Available online at www.sciencedirect.com
SCIENCE DIRECT®
Journal of the European Ceramic Society 25 (2005) 3301–3306
www.elsevier.com/locate/jeurceramsoc

Structural and electrical properties of aluminum-doped zinc oxide films prepared by sol–gel process

Radhouane Bel Hadj Tahar *

Département de Physique Chimie, Institut Préparatoire aux Etudes d'Ingénieurs de Sfax, Université du Sud, B. P. 805 Sfax 3000, Tunisie, Tunisia

Received 3 July 2004; accepted 19 August 2004
Available online 6 June 2005

Abstract

Aluminium-doped zinc oxide films were prepared through a non-alkoxide dip-coating technique from zinc acetate and aluminium nitrate in alcoholic solution. The doping concentration in the films varied between 0 and 8 at.%. The structural and electrical properties of the Al-doped zinc oxide (AZO) films are investigated in terms of the preparation conditions, such as the Al content, precursor solution, firing and annealing temperatures. The crystal structure of the AZO films is hexagonal wurtzite. In the present study, we found that the critical parameter determining the crystal quality is the aluminum concentration. The crystallographic orientation depends on the precursor system used in the film preparation regardless of the Al content and the heat-treatment temperature. The resistivity of the 1 at.%-doped AZO film is $2.5 \times 10^{-3}\ \Omega$ cm and depends mainly on the electronic mobility.

Keywords: ZnO; Films; Electrical properties; Sol–gel processes

1. Introduction

Zinc oxide (ZnO) is a wide-band-gap semiconductor (3.3 eV). Like indium oxide and tin oxide, ZnO is both transparent in the visible region and electrically conductive especially when doped with appropriate metals such as indium,[1,2] gallium,[3] or aluminum. This unique property has been widely studied for its practical applications such as transparent conducting electrodes for flat panel displays, and solar cells.[4]

Al-doped zinc oxide films can be prepared by numerous techniques such as radio-frequency magnetron sputtering,[5] chemical vapor deposition,[6] and thermal evaporation.[7] However, these techniques require sophisticated instruments and/or a high-temperature deposition. Therefore, if highly conductive and transparent AZO films could be made with an inexpensive deposition technique, the films could be a potential low-cost alternative to the widely used tin-doped indium oxide (ITO).[8] In this respect, deposition processes based on sol–gel chemistry would offer the possibility of large area coating and intimate mixing of the starting materials which results in high degree of film homogeneity, yet do not incur high capital equipments. Despite these advantages, relatively few reports deal with the sol–gel preparation of AZO transparent conductors. Most of the work has been done on AZO thin films deposited mainly by physical methods. Coatings with satisfactory electrical conductivities have been successfully deposited by sputtering. On the other hand, one order low values are reported for the sol–gel coated films. However, the reasons for these low conductivity values as well as the dependence of the electrical properties on the preparation technique have not been elucidated, probably because of the complex structure of zinc oxide and the number of parameters involved even for a single film processing technique.

In this article we present a detailed account of the sol–gel growth of AZO semi-conducting coatings. This study serves two main purposes: to correlate the depositing parameters with the film structural and physical properties, and to

* Fax: +216 74 246 347.
E-mail address: belhadjtahar2001@yahoo.com.

0955-2219/$ – see front matter © 2004 Published by Elsevier Ltd.
doi:10.1016/j.jeurceramsoc.2004.08.028

elucidate the reasons for the relatively low conductivities obtained for the sol–gel deposited films. Few suggestions are included in order to further improve the electrical properties of these films. The structural characterization of the layers is also described.

2. Experimental

Two sol–gel categories have been used to deposit AZO thin films: (i) processes based on the use of the solvent 2-methoxyethanol[9,10] (in the following designated as precursor 1): and (ii) processes based on chelating ligands such as ethanolamine[11–15] compounds (precursor 2). A solution of ZnO precursor was made by dissolving zinc acetate [$Zn(CH_3CO_2)_2{\cdot}2H_2O$] in either isopropanol or methoxyethanol depending on the precursor system being used. The stability of the process is set by control of the hydrolysis and condensation reactions such that they take place only when the solution dries, solvent is lost or temperature is elevated. Therefore, diethanolamine (DEA) or monoethanolamine (MEA) were added as chelating ligands to improve the precursor solubility. The optimum amount of additive in the system provided a homogeneous distribution of the metal ions and prevented their precipitation from the solution prior to thermal treatment. The solution was then hydrolyzed with 2 mol H_2O per mol metal acetate to improve the wetness and uniformity of the coating on the substrate. To achieve aluminum doping, aluminum nitrate [$Al(NO_3)_3{\cdot}9H_2O$] was added to the solution. AZO films were prepared by dip coating the stock solution onto substrates (Corning 7059, Corning Glass Works, Coming, NY, USA). After coating, the substrates were dried at 100 °C for 10 min and loaded carefully into an electrically heated tube furnace held at the desired temperature. The above process of coating and firing was repeated several times to increase the thickness of the films. Selected samples were subsequently heated in vacuum (10^{-3} Torr) at different temperatures to investigate the effect of annealing on the electrical properties and optical spectra. The structural development of the films was investigated by X-ray diffraction (XRD) patterns, which were recorded using Cu Kα radiation. The scanning range was between $2\theta = 20$ and 70°. The average crystallite size for a series of heat-treated ZnO and AZO films were calculated from the X-ray ($d_{0\,0\,2}$) line broadening using Scherrer's equation. The correct XRD peak profiles were measured in the step-scan mode with a step interval of 0.02° 2θ. Standard silicon powder that was made from silicon single-crystal wafers was used as an internal standard. The chemical processes which occur during the drying and the oxide formation were followed by simultaneous thermogravimetric and differential thermal analysis (TG/DTA). For all the runs, rising temperature experiments were conducted in the temperature range from ambient to 1000 °C at a heating rate of 5 °C/min. The electrical resistivity and Hall coefficient of the films were measured at room temperature by van der Pauw methods.

3. Results and discussion

3.1. Thermo-gravimetric and differential thermal analysis

Knowledge of the different bulk transformations that occur on sintering can assist interpretation of certain film properties. However, one should note that the TG/DTA results should not be directly extrapolated to the case of a film, because they were recorded on gel powders and at a slow heating rate, whereas the films prepared in this study were directly heated at a given temperature. Fig. 1 shows the TG/DT curves of pure and aluminum-doped (2 at.% Al) zinc oxide gel powders. The TG curve indicates that the evaporation of residual solvent and diethanolamine occurs between 100 and 270 °C. The pyrolysis of residual organics is basically characterized by an exothermic process which occurs between 270 and 410 °C. The exothermic decomposition of the carbonaceous DEA (or MEA) results in high in situ temperatures. As a result, The AZO phase formation occurs at a relatively lower external temperatures (400 °C for 30 min) through this route, in comparison to all the other reported chemical routes (except hydrothermal). Analysis of XRD measurement suggests that the broad exothermic peak at 410–500 °C is associated with the formation and crystallization of zinc oxide phase. The broad exothermic peak at 550 °C that is observed only for Al-doped powders is probably attributed to the formation crystallization of Al_2O_3 since it appears only at relatively high doping concentration ($\geq$ 2 at.% Al) and it is not accompanied with a weight loss. This could not be confirmed by XRD possibly because the amount of Al_2O_3 is below the detection limit of the instrument. The eventual influence of Al_2O_3 on the film electrical properties will be further discussed in the following sections. The entire thermal effect was accompanied by the evolution of gases (such as CO, CO_2, and water vapor) that was manifested in a total weight loss of 68% in the TG curve.

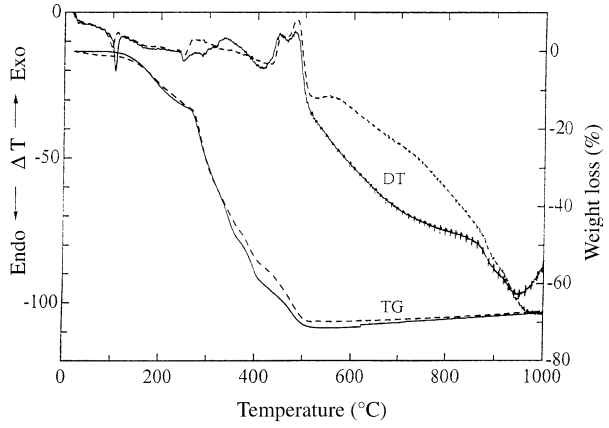

Fig. 1. Typical TG/DT curves measured in air at a heating rate of 5 °C/min for pure (solid curves) and 2 at.% Al (dashed curves) doped zinc oxide gel powders that were prepared from precursor 2.

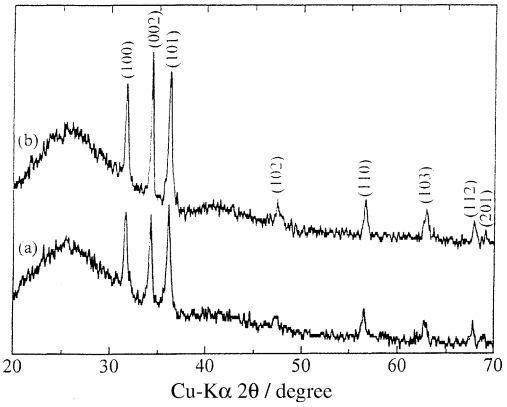

Fig. 2. X-ray diffractograms for air-annealed AZO films (0.3 at.% Al, 450 °C) that were prepared from isopropanol–DEA system (a) before and (b) after vacuum annealing at 450 °C for 1 h.

3.2. Structural characterization

Films grow to minimize the surface free energy. If the surface free energy of a plane is lower than that of other planes, the films grow with the plane of lower surface free energy.[16] In the case of ZnO crystal, the surface energy density of the (0 0 2) orientation is the lowest.[17] Grains with lower surface energy will become larger as the film grows. Then the growth orientation develops into one crystallographic direction of the lowest surface energy. This means that (0 0 2) texture of the film may easily form. The *c*-axis orientation in AZO films can also be understood by the "survival of the fastest" model proposed by Drift.[18] According to this model, nucleations with various orientations can be formed at the initial stage of the deposition and each nucleus competes to grow but only nuclei having the fastest growth rate can survive, i.e., *c*-axis orientation is achieved.

The X-ray data have been studied for films that were prepared from precursors 1 and 2, before and after annealing (Figs. 2 and 3). As clearly seen from Figs. 2 and 3, perfectly oriented films with the (0 0 2) axis normal to the amorphous substrate surface are obtained from precursor 1, while contrary to what is expected, randomly oriented AZO films are prepared from precursor 2. The random orientation obtained in films from precursor 2 clearly indicates the strong influence of the chemical physical characteristics of the solution on the film final structure. This result is quite interesting since it demonstrates that the crystallite orientation can simply and intentionally be tailored by choosing an adequate solvent-chelating ligand combination. Although it has been demonstrated[19] that the crystallographic orientation does not play a significant role in the electrical properties of AZO thin films, the easiness of producing highly oriented coatings by sol–gel technique may find important applications in fields other than transparent conductors such as in ferroelectric and piezoelectric coatings where the microstructure is known to have a strong influence on the dielectric properties of these materials. Therefore, the preparation of highly oriented coatings on amorphous substrates by sol–gel technique and the understanding of the role of the different parameters that are involved is an interesting research area that should be further explored.

The X-ray difrractograms for AZO films of varying aluminum content are illustrated in Fig. 4. These spectra show rather broad diffraction peaks at positions consistent with the bulk wurtzite crystal structure. No metallic zinc crystallite structure was detected. Fig. 4 also shows a drastic degradation of the film crystallinity at high dopant concentration. XRD studies of heat-treated AZO dried gel powders were also performed. The final product was assumed to have aluminum incorporated homogeneously into the zinc oxide matrix, because no extra lines were observed in the XRD patterns of AZO powders in the studied range of aluminum concentration (0–8 at.% Al).

The calculated values of the crystallite sizes for selected samples are depicted in Table 1. The mean crystallite size values drastically fall as the aluminum doping increases (runs 1–4). Despite being highly oriented, comparable crystallite size values are also obtained for the films that were prepared from precursor 1 (runs 8–10). Doubling the film thickness slightly increased the crystallite size from 18 to 27 nm for

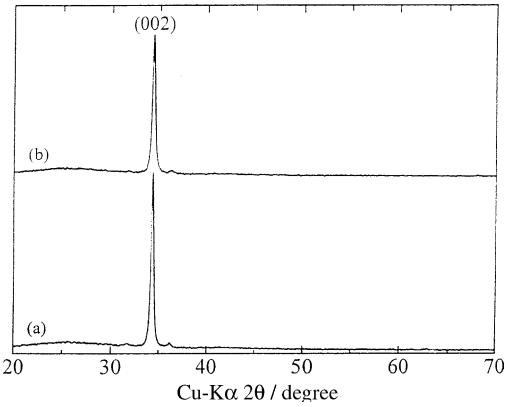

Fig. 3. X-ray diffractograms for air-annealed AZO films (0.7 at.% Al, 450 °C) that were prepared from methoxyethanolnol–MEA system (a) before and (b) after vacuum annealing at 450 °C for 1 h.

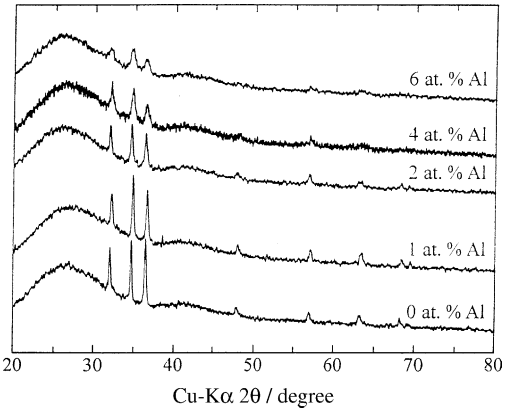

Fig. 4. X-ray diffractograms for AZO films as a function of aluminum content. The films were prepared from precursor 2 and fired at 650 °C for 30 min.

Table 1
Variation of the crystallite size, carrier mean free path, and refractive indices of the AZO films with the coating conditions

Run	Coating conditions					Crystallite size (nm)		Carrier mean free path (nm) (annealed films)	Film thickness (nm)	Refractive index
	Precursor	Al concentration (at.% Al)	Application number	Deposition temperature (°C)	Annealing temperature (°C)	As-deposited	Annealed			
1	2	0.0	10	450	450	72	66	3.2	237	1.82
2	2	0.3	10	450	450	51	–	3.7	227	1.82
3	2	0.7	10	450	450	41	36	6.0	239	1.74
4	2	1.0	10	450	450	18	–	4.6	261	1.74
5	2	2.0	10	450	450	–	–	2.0	261	1.75
6	2	3.0	10	450	450	–	–	1.5	229	1.71
7	2	1.0	20	450	450	27	–	–	477	1.76
8	1	0.3	10	450	450	39	–	6.9	197	1.81
9	1	0.7	10	450	450	39	33	10.2	–	–
10	1	1.0	10	450	450	19	–	5.1	176	1.94

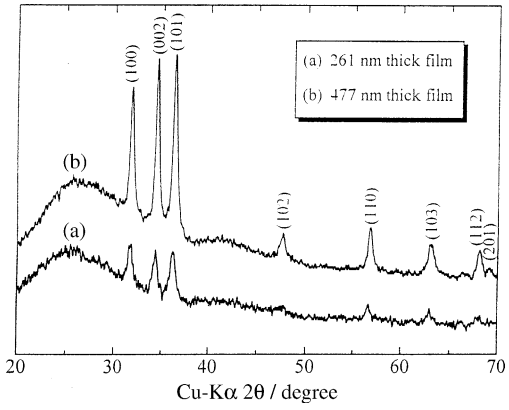

Fig. 5. X-ray diffractograms for AZO films (0.3 at.% Al, 450 °C) prepared from precursor solution 2 as a function of the thickness.

the 477 nm thick film (runs 4 and 7) but did not change the crystallographic orientation as clearly seen in Fig. 5. It is also observed that the crystallite size values normal to the substrate plane of the as-deposited AZO films slightly change on vacuum annealing.

From the above results it can be concluded that, once the firing and annealing temperatures are optimized, the main parameters affecting the crystal growth in the present sol–gel deposited AZO films are the precursor system from which the films are prepared and the aluminum doping concentration. Varying the precursor system probably affects the surface free energy of the crystallographic planes and/or the growth rate of nuclei leading to the fabrication of films with different orientations. Conversely, the dopant aluminum tends to create more nucleation centers during the deposition process and as a consequence the doped films have small crystallite sizes.

3.3. Electrical characteristics

The electrical properties of the oxides depend critically upon the oxidation state of the metal component (stoichiometry of the oxide) and on the nature and quantity of impurities incorporated in the films, either intentionally or inadvertently.[20] Oxygen vacancies occupied with two electrons as well as zinc interstitials are the two types of defects responsible for the n-type conductivity in pure zinc oxide. The electrical conductivity in AZO films is essentially due to the contribution from Al^{3+} ions on substitutional sites of Zn^{2+} ions and Al interstitial atoms as well as from oxygen vacancies and Zn interstitial atoms. The specific gravity of zinc oxide is 5.72 g/cm^3, corresponding to 4.21×10^{22} molecules per cm^3.[21] Therefore, the theoretical carrier density (n) calculated under the assumption that every dissolved Al atom supplies one free electron to the conduction band is demonstrated by the equation: $n = 4.2 \times 10^{20} \times C_{Al}$, where C_{Al} is the aluminum concentration (at.% Al). However, practically, the earner concentration does not increase as expected.

Table 2 shows how the electrical resistivity (ρ), Hall mobility (μ_H), and carrier concentration (n) of AZO films are related to the aluminum content and the precursor solution. All the samples were prepared at the same deposition conditions. The carrier concentration for pure ZnO film is 0.76×10^{19}/cm^3, but those for AZO films ($C_{Al} \geq 1$ at.%) are more than 10^{20}/cm^3, implying that the deposited AZO films are degenerate semiconductors. As the dopant concentration increases, the carrier density increases but it saturates at 5.6×10^{20}/cm^3 for Al doping levels higher than 2 at.%. The above behavior of n suggests that not all the Al atoms in the film contribute to dopants: an increasing amount of Al remains electrically inactive above 1 at.%. In fact the doping efficiency, defined as the ratio of the number of free electron in the film to the aluminum concentration, gives the fraction of aluminum atoms that are electrically active which does not exceed 44% for the 3 at.% doped film. This can be explained by the formation of neutral impurities[19] such as nonconductive aluminum oxide from the extra aluminium atoms. The extra aluminum atoms might not occupy the correct places inside the zinc oxide crystallites because of the limited solubility of aluminum inside ZnO matrix. Another particularly

Table 2
Variation of the electrical properties of the AZO films with the dopant concentration and precursor system

Coating conditions						Electrical properties of annealed films			Doping efficiency[a] (%)
Precursor	Al concentration (at.%)	Application number	Coating rate (cm/min)	Deposition temperature (°C)	Annealing temperature (°C)	Resistivity ($\times 10^3\ \Omega$ cm)	Carrier concentration ($\times 10^{20}$/cm^3)	Hull mobility (cm^2/V s)	
2	0.0	10	6	450	450	14.1	0.76	5.9	–
2	0.3	10	6	450	450	11.3	0.84	6.6	67
2	0.7	10	6	450	450	6.6	0.90	10.5	31
2	1.0	10	6	450	450	3.6	3.33	5.1	79
2	2.0	10	6	450	450	5.9	5.63	1.9	67
2	3.0	10	6	450	450	8.1	5.60	1.4	44
1	0.3	10	6	450	450	5.2	1.05	11.4	83
1	0.7	10	6	450	450	3.4	1.11	16.4	38
1	1.0	10	6	450	450	2.5	4.89	5.5	116

[a]Ratio of measured carrier concentration to that calculated under the assumption that every dissolved Al atom supplies one free electron: $n \times 100/4.2 \times 10^{20}\ C_{Al}$.

important cause for the relatively low carrier densities is the porous nature of the sol–gel coated AZO films (low refractive indices, Table 1) which facilitates oxygen indiffusion.[22] Moreover, since the ionic radius of aluminum (0.56 Å) is smaller than that of zinc (0.74 Å), the excess of aluminum may occupy interstitial positions and distort the crystal structure which may negatively affect the electronic mobility. The relatively low efficiencies reported in the present work, especially for the highly doped films, indicate that the post-deposition treatment is not quite efficient. A systematic study on the electrical properties of AZO films as a function of the oxygen partial pressure during the annealing step is underway.

The electronic mobility is diminished by any type of disturbance of the periodic lattice potential.[23] There are many sources of electron scattering which may influence the electrical and optical properties of the AZO films. Grain boundaries, ionized point defects, and neutral impurities are the major scattering centers. The room-temperature Hall mobilities measured for lightly doped single-crystal ZnO are typically around 180 cm^2/V s[24] whereas those measured for the present films do not exceed 17.0 cm^2/V s. These mobility values are modest even when compared to those of sputtered polycrystalline films.

From boundary scattering, the electron mean free path L is described using a highly degenerate electron gas model[25]:

$$L = (3\pi^2)^{1/3}(h\,e^{-2})\rho^{-1}n^{-2/3}$$

The calculated values of L and the crystallite size of selected samples are listed in Table 1. This table clearly shows that scattering by grain boundaries apparently play a subordinate role in the present films since the carrier mean free path is considerably shorter than the average crystallite. Radhouane et al.[19,26] have demonstrated that the behavior of the electron mobility in sol–gel coated AZO films can be interpreted in terms of neutral and ionized impurity scattering. Kim et al.[27] reported that the carrier concentration decreases from 7.5×10^{20}/cm^3 for the AZO sputtered film prepared with the 3 wt.% Al_2O_3 target to $\sim 2.4 \times 10^{20}$/cm^3 for sample prepared with the 5 wt.% Al_2O_3 target. Unexpectedly, this was accompanied by a sharp decrease in the electron mobility from $\sim$20 to 2 cm^2/V s. They concluded that the carrier mobility of their sputtered films is dominated mostly by grain boundary scattering rather than by ionized impurity scattering. However, considering the grain boundaries as the main damping mechanism of the free electrons in highly Al-doped zinc oxide seems unlikely since the mean free path (L) for these sputtered films is clearly smaller than the reported crystallite size values. At high doping levels exceeding the solubility limit, the excess aluminum atoms do not activate but rather form electrically inactive impurities which impair the mobility and carrier concentration. Therefore, regardless of their nature and composition, the concentration of these neutral impurities should be minimized to ameliorate the conductivity of AZO films. On the other hand, the scattering by ionized centers can not be avoided since high carrier densities are required.

The slightly higher mobility and carrier concentration values that are measured for the films deposited from precursor 1 in comparison with those from precursor 2 lead to a minimum resistivity of 2.5×10^{-3}. This is due to the higher density of these films (higher refractive index, see Table 1) rather than the crystallographic orientation as previously pointed out.[19] The optimum resistivity obtained in the present study ($2.5 \times 10^{-3}\ \Omega$ cm) is still one order higher than that obtained for films deposited by physical techniques such as sputtering. This is mainly due to the difference between the physical and sol–gel film deposition techniques; that is the possibility of controlling the oxygen content in the film during deposition. The oxygen concentration can easily be controlled in the former methods whereas it is difficult to adjust it for the sol–gel technique since there is an inevitable contribu-

tion from the organic compounds present in the green film. This will have an important repercussion on the film electrical properties since the degree of oxidation is a crucial parameter that determines the carrier concentration and mobility of non-stoichiometric and doped films of several oxides. This implies that post-annealing treatment under reduced atmospheres is often required for sol–gel deposited coatings. The discrepancies of the conductivity values quoted in the literature for the sol–gel deposited films is in direct relation with the post-annealing conditions namely the oxygen partial pressure values which are not even mentioned in most of the published articles. The oxygen partial pressure during annealing treatment should be low enough to activate donors through the decrease in the density of neutral impurities, and not only by creating oxygen vacancies, and to facilitate the out-diffusion of oxygen without precipitating the doping metal. Another important factor is the depositing temperature that should be optimized to avoid the formation and in a next stage the crystallization of the dopant oxide because this will electrically deactivate it and complicate the annealing procedure.

4. Conclusions

The results presented in this study show the sol–gel process to be feasible for the deposition of oriented ZnO-based films. (0 0 2)-oriented polycrystal films are deposited on amorphous glass substrates using a suitable starting solution. The structural properties of the films appear to be highly dependent upon the precursor solution and the doping level. The X-ray diffraction peaks broadened as the aluminium content was increased, indicating smaller grain size with high doping concentration. High aluminum content in the films does not always increase the free-electron concentration since aluminum atoms must replace zinc atoms inside the crystallites to generate conduction electron. The present results suggest that post-annealing treatment at low oxygen pressure ($\sim 10^{-5}$ Torr) is one possible means for obtaining improved sol–gel deposited films since the out-diffusion of excess oxygen atoms reactivates aluminum atoms which might exist within neutral complexes in addition to the creation of oxygen vacancies.

References

1. Nunes, P., Malik, A., Fernandes, B., Fortunate, E., Vilarinho, P. and Martins, R., *Vacuum*, 1999, **52**, 45.
2. Szyszka, B. and Jäger, S., *J. Non-Cryst. Solids*, 1997, **218**, 74.
3. Cook, B. A., Harringa, J. L. and Vining, C. B., *J. Appl. Phys.*, 1998, **83**, 5858.
4. Jin, Z.-C., Hamberg, I. and Granqvist, C. G., *J. Appl. Phys.*, 1988, **64**, 5117.
5. Cebulla, R., Wendt, R. and Ellmer, K., *J. Appl. Phys.*, 1998, **83**, 1089.
6. Hu, J. and Gordon, R. G., *J. Appl. Phys.*, 1992, **71**, 880.
7. Ma, J., Ji, F., Ma, H.-l. and Li, S.-y., *Sol. Energy Mater. Sol. Cells*, 2000, **60**, 341.
8. Bel Hadj Tahar, R., Ban, T., Ohya, Y. and Takahashi, Y., *J. Appl. Phys.*, 1997, **82**, 865.
9. Ohyama, M., Kozuka, H., Yoko, T. and Sakka, S., *Jpn. J. Ceram. Soc.*, 1996, **104**, 296.
10. Kozuka, H. and Yoko, T., *J. Am. Ceram. Soc.*, 1998, **81**, 1622.
11. Ohya, Y., Saiki, H. and Yakahashi, Y., *J. Mater. Sci.*, 1994, **29**, 4099.
12. Ohya, Y., Saiki, H., Tanaka, T. and Takahashi, Y., *J. Am. Ceram. Soc.*, 1996, **79**, 825.
13. Bel Hadj Tahar, R., Ban, T., Ohya, Y. and Takahashi, Y., *J. Am. Ceram. Soc.*, 1998, **81**, 321.
14. Takahashi, Y., Okada, S., Bel Hadj Tahar, R., Nakano, K., Ban, T. and Ohya, Y., *J. Non-Cryst. Solids*, 1997, **228**, 129.
15. Bel Hadj Tahar, R., Ban, T., Ohya, Y. and Takahashi, Y., *J. Am. Ceram. Soc.*, 2001, **84**, 85.
16. Goto, S., Fujimura, N., Nishihara, T. and Ito, T., *J. Cryst. Growth*, 1991, **115**, 816.
17. Chopra, K. L., Major, S. and Pandaya, D. K., *Thin Solid Films*, 1983, **102**, 1.
18. Van der Drift, A., *Philips Res. Rep.*, 1967, **22**, 267.
19. Bel Hadj Tahar, R. and Bel Hadj Tahar, N., *J. Appl. Phys.*, 2002, **92**, 4498.
20. Bel Hadj Tahar, R., Ban, T., Ohya, Y. and Takahashi, Y., *J. Appl. Phys.*, 1998, **83**, 2631.
21. Neumann, G., *Current Topics in Materials Science, Vol. 7*, ed. E. Kaldis. North Holland, Amsterdam, 1981, p. 154.
22. Castro, M. S. and Aldao, C. M., *J. Eur. Ceram. Soc*, 1999, **19**, 511.
23. Hirschwald, W., Bonasevvicz, P., Ernst, L., Grade, M., Hofmann, D., Krebs, S. *et al.*, *Current Topics in Materials Science, Vol. 7*, ed. E. Kaldis. North-Holland, Amsterdam, 1981 (Chapter 3).
24. Lide, D. R., *Handbook of Chemistry and Physics* (*71st ed.*). CRC, Boca Raton, FL, 1991.
25. Kittel, C., *Introduction to Solid State Physics* (*5th ed.*). Maruzen, Tokyo, 1985, Chap. 6.
26. Bel Hadj Tahar, R., Ban, T., Ohya, Y. and Takahashi, Y., *J. Appl. Phys.*, 1998, **83**, 2139.
27. Kim, K. H., Park, K. C. and Ma, D. Y., *J. Appl. Phys.*, 1997, **81**, 7764.